Phonon scattering effects on thermal conductivity of TiNiSn-based half-Heusler alloys

S. Bhattacharya,[a,]* T. M. Tritt[a], M. J. Skove[a], M. Russell[a], S. J. Poon[b], V. Ponnambalam[b], Y. Xia[b], N. Thadhani[c]

[a] *Dept. of Physics, Clemson University, Clemson, SC 29634. Tel: 864 656 5319; E-mail: ttritt@clemson.edu*
[b] *Dept. of Physics, University of Virginia, Charlottesville, VA 22901. Tel: 434 924 6793; E-mail: sb7uj@virginia.edu (corresponding author)**
[c] *Materials Science and Engineering, GA Institute of Technology, Atlanta, GA 30332. E-mail: naresh.thadhani@mse.gatech.edu*

Received July 31, 2008

TiNiSn-based half-Heusler alloys have been of significant interest for their potential as thermoelectric materials, which arises from their promising electronic transport properties. They exhibit high Seebeck coefficients and moderate electrical resistivity values but have comparatively high lattice thermal conductivities (κ_L) that need to be reduced. A significant reduction in κ_L with substitutions of large concentrations of Zr ($y \geq 25\%$) in $Ti_{1-y}Zr_yNiSn_{0.95}Sb_{0.05}$ is observed and attributed to mass fluctuation scattering. In contrast, minute amounts of Sb-doping ($x \leq 5\%$) at the Sn-site in $TiNiSn_{1-x}Sb_x$ gives rise to non-systematic increase in κ_L. Extensive micro-structural analysis indicate a correlation between κ_L and the average grain diameter of these materials. The two different phonon scattering mechanisms to reduce κ_L are discussed in the Ti and Zr-based half-Heusler alloys.

1. Introduction

Over the past few decades, there has been a revived interest in the field of thermoelectricity. New and advanced thermoelectric (TE) materials have been investigated as an alternate mode of energy conversion for refrigeration and power generation applications[1,2,3]. Power generation systems with radioactive thermoelectric generators (RTGs) used by NASA in the deep space missions of the Voyager I and II and the Cassini Mission to Saturn have proved to be highly reliable and long lasting. TE materials and devices are of interest for their reliability and durability, and the technology is also environment friendly and ecologically safe. The simplicity and compactness of a TE generator with no moving parts (a solid state device) makes it ideal for niche applications.

The efficiency of a TE material is determined by the dimensionless parameter ZT, also known as the figure of merit of the TE material and is given by[4]:

$$ZT = \frac{\alpha^2 \sigma T}{\kappa} \qquad (1)$$

where, α is the Seebeck coefficient or thermopower, σ (= $1/\rho$) is the electrical conductivity and ρ the electrical resistivity, κ (= $\kappa_L+\kappa_E$) is the thermal conductivity, comprised of the lattice (κ_L) and electrical contributions (κ_E). The state-of-the-art TE materials are Bi_2Te_3 (ZT ≈ 1 at 350 K) and SiGe (ZT ≈ 1 at T = 1200 K) [5]. The goal is to find new TE materials that would exhibit a higher efficiency (ZT ~ 2-3) over a broader range of temperature.

An ideal TE material exhibits high Seebeck coefficient ($\alpha \approx 100 - 300\ \mu V\ K^{-1}$) and favorable electrical conductivity ($\sigma \approx 10^2 - 10^4\ \Omega\text{-cm}^{-1}$) as observed in semi-metals or semiconductors with an optimal energy gap ($E_g \approx 0.25$ eV).[6] Optimizing the Seebeck coefficient and electrical conductivity simultaneously via "doping" or chemical substitution also improves the electronic transport properties. To maximize ZT further, methods to "tune" the lattice thermal conductivity by increasing phonon scattering via mass fluctuation or grain boundary scattering have been investigated [7,8].

In recent years, attention has been focused on the TiNiSn based half-Heusler alloys for their potential as thermoelectric materials. The half-Heusler alloys are a group of ternary intermetallic compounds that exhibit the cubic MgAgAs ($C1_b$) crystal structure[9,10]., MNiSn (M= Hf, Zr, Ti) half-Heusler alloys possess three filled and one vacant interpenetrating fcc sublattices with twelve atoms in a unit cell. They are structurally comparable to their parent compounds, the Heusler alloys (MNi_2Sn) that have all the four sub-lattices occupied by Ni atoms. The presence of a narrow bandgap in the half-Heusler alloys accounts for the "tunability" and variability of the electrical resistivity ($\rho \approx 1/\sigma \approx$ 0.1-8 mΩ-cm) at room temperature. The combination of the high negative thermopower ($\alpha >> 150\ \mu V/K$) and low electrical resistivity results in a power factor as high as ($\alpha^2\sigma T \approx 1.0\ Wm^{-1}K^{-1}$) at room temperature. A very large power factor ($\alpha^2\sigma T$) of about 4.5 $Wm^{-1}K^{-1}$ at 650 K has been reported in the $TiNiSn_{0.95}Sb_{0.05}$ half-Heusler alloy[11]. Other groups have also reported promising transport properties in the half-Heusler alloys. A ZT ≈ 0.7 at 800 K in $Zr_{0.5}Hf_{0.5}Ni_{0.8}Pd_{0.2}Sn_{0.99}Sb_{0.01}$ has been reported in the half-Heusler alloys by Shen *et al*[12]. The highest value of ZT = 0.81 at T = 1025 K was observed by Culp *et al*[13]. in half-Heusler alloys with the composition $Hf_{0.75}Zr_{0.25}NiSn_{0.975}Sb_{0.025}$, which was found to exceed the standard set for industrial purposes by the SiGe alloys.

2. Experimental procedure

Alloys of different compositions were synthesized at the University of Virginia by arc-melting appropriate quantities of elements together. For a "standard" alloy, short term annealing at 900 °C for 14 h and long term annealing at week was carried out. Ball-milling at UVA was performed on an as-cast ingot to ensure particle control and the process is also known to produce nano-sized particles (clusters). The ball-milled powders were shock consolidated using a three-capsule plate-impact compaction

fixture, with a single stage gas gun at GA Tech. This process discourages further grain growth. Details of synthesis and shock-compaction procedures are found elsewhere.[Error! Bookmark not defined.,Error! Bookmark not defined.] Resistivity and thermopower were measured simultaneously at Clemson University in a closed cycle helium cryostat from 10 to 300 K and the specific technique is described in detail elsewhere[14]. The thermal conductivity was also measured from 10 to 300 K using a separate custom designed system using a steady state technique. The mounting and measurement technique and instrumentation are also described in detail elsewhere.

2. Results and Discussion

Athough the TiNiSn half-Heusler alloys exhibit promising electrical transport properties, the lattice thermal conductivity measured (≈10 $Wm^{-1}K^{-1}$ at 300 K) is quite high and is an important physical property to optimize. The thermal conductivity in half-Heusler alloys consists chiefly of the lattice 750°C for one

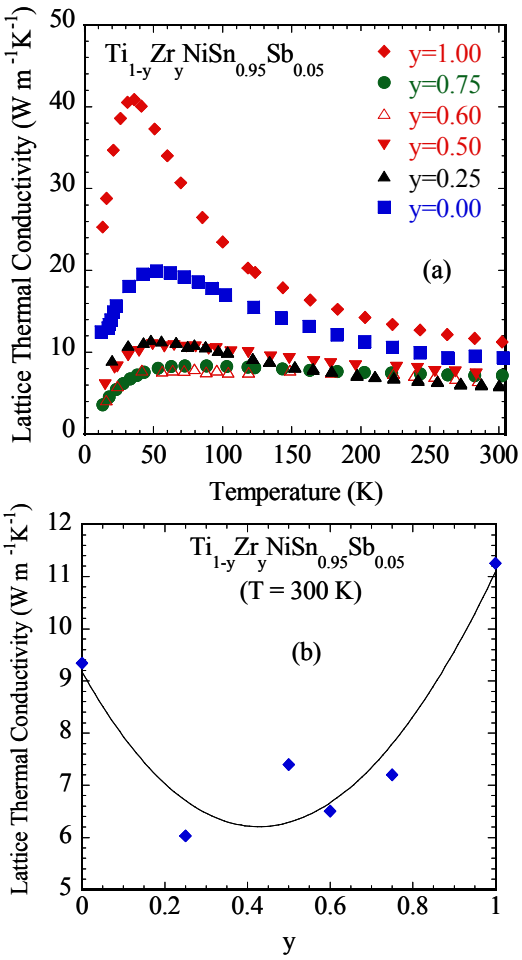

Figure 1: Lattice thermal conductivity vs. (a) Temperature (b) nominal concentration of Zr substitution, in the $Ti_{1-y}Zr_yNiSn_{0.95}Sb_{0.05}$ series.

contribution ($\kappa_L \approx 90\%$ of the total κ_T), calculated indirectly using the Wiedemann Franz relation ($\kappa_E = L_O \sigma T$, where L_O = 2.45 x 10^{-8} V^2/K^2 is the Lorenz number, and ($\kappa_L = \kappa_T - \kappa_E$)).

At higher temperatures (T ≥ 200 K), κ_L is typically dominated by phonon-phonon interactions which limit the phonon mean free path ℓ_{ph}, causing κ_L to exhibit a 1/T dependence. At these temperatures, the velocity of sound (v_s) or phonon velocity and the specific heat capacity per unit volume of phonons (c_v) are essentially a constant, where $\kappa_L = \frac{1}{3} c_v v_s \ell_{ph}$. Hence, κ_L may be reduced by increasing phonon scattering mechanisms such as phonon-phonon interactions, scattering by grain boundaries (both external and internal), point defects, impurities, isotopes, dislocations etc[15].

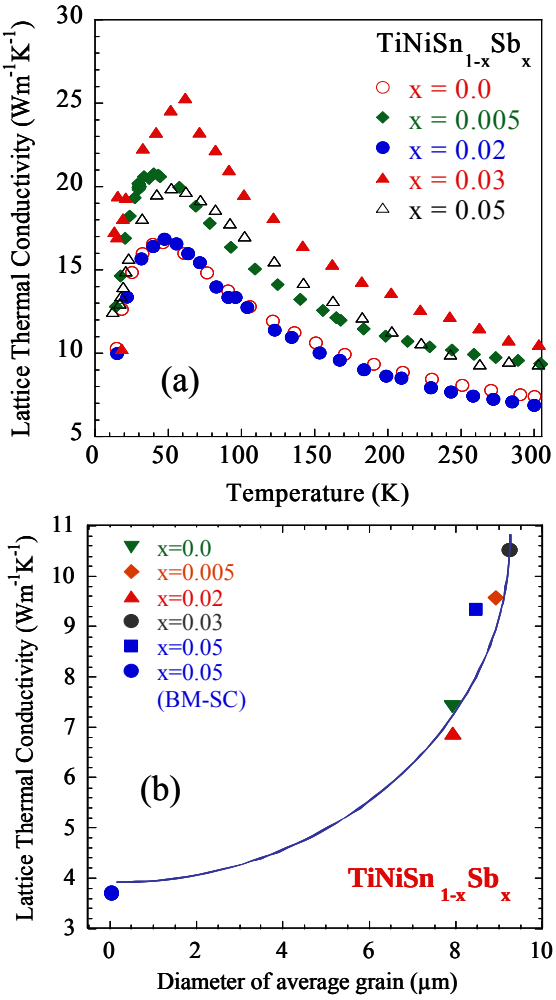

Figure 2: Lattice thermal conductivity *vs* temperature (b) average grain diameter in $TiNiSn_{1-x}Sb_x$ series at 300 K.

The effect of substituting large concentrations of Zr (≥ 20%) at the Ti site in the $Ti_{1-y}Zr_yNiSn_{0.95}Sb_{0.05}$ series was studied, keeping the optimal Sb-doping (5%) a constant. The electronic transport properties in the $Ti_{1-y}Zr_yNiSn_{0.95}Sb_{0.05}$ series exhibit the upper limits of power factors ($\alpha^2\sigma T$) in the parent compositions $TiNiSn_{0.95}Sb_{0.05}$ and $ZrNiSn_{0.95}Sb_{0.05}$, decreasing in magnitude with increasing Zr substitution at the Ti site. $TiNiSn_{0.95}Sb_{0.05}$, remains the optimal composition in this series of samples with the highest power factor (≈ 1.0 $Wm^{-1}K^{-1}$ at T = 300 K).[15] Figure 1(a) shows κ_L as a function of temperature for the series, $Ti_{1-y}Zr_yNiSn_{0.95}Sb_{0.05}$, (y = 0.0, 0.25, 0.5, 0.6, 0.75

and 1.0). The end elements of the series, $ZrNiSn_{0.95}Sb_{0.05}$ and $TiNiSn_{0.95}Sb_{0.05}$ exhibit the highest κ_L values, while κ_L in the intermediate alloyed compounds $Ti_{1-y}Zr_yNiSn_{0.95}Sb_{0.05}$ (y = 0.25, 0.5, 0.6 and 0.75) are highly reduced by almost 50%, most likely due to mass fluctuation scattering arising from the difference in the atomic masses of Zr (M_{Zr} = 91 g/mol) and Ti (M_{Ti} = 48 g/mol). Figure 1 (b) shows κ_L at 300 K *vs.* Zr concentration (y), with a maximum mass disorder and a reduction of κ_L near a concentration of 50 % Zr at Ti site, pointing towards mass fluctuation scattering.

Figure 2(a) shows κ_L *vs.* temperature in the $TiNiSn_{1-x}Sb_x$ series with minute (x≤ 5%) amounts of Sb doping at Sn-site. Pure TiNiSn exhibits a thermal conductivity of about 8 $Wm^{-1}K^{-1}$ at room temperature, in good agreement with the thermal conductivity of TiNiSn measured by other groups (9 $Wm^{-1}K^{-1}$ at 300 K)[16]. For these low concentrations of Sb doping in the $TiNiSn_{1-x}Sb_x$ (x = 0.0, 0.005, 0.02, 0.03, 0.05), the room temperature values of thermal conductivity vary non-systematically over a range from approximately (6 – 15) $Wm^{-1}K^{-1}$, although it is expected that κ_L in this series would be of similar magnitudes at all temperatures due to the close proximity of Sb (M_{Sb} = 121.8 g/mol) and Sn (M_{Sn} = 118.7 g/mol) in the periodic table.

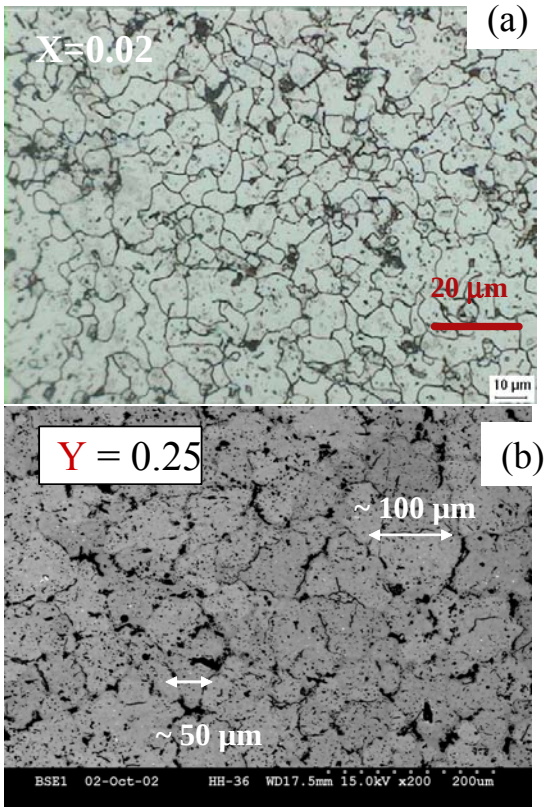

Figure 3: Characteristic grain structures in (a) $TiNiSn_{1-x}Sb_x$ (x = 0.02) (D ≤ 10 µm) and(b) $Ti_{1-y}Zr_yNiSn_{0.95}Sb_{0.05}$ (y = 0.25) (D ≥ 50 µm)

Extensive micro-structural studies in the $TiNiSn_{1-x}Sb_x$ series have established a direct correlation of κ_L with the average grain diameter (D) in these materials as shown in figure 2(b).[Error! Bookmark not defined.] For the "standard" $TiNiSn_{1-x}Sb_x$ compounds specified earlier, κ_L decreases systematically with a decrease in grain diameter (D ≤ 10 µm) even with the small variations of grain size. This plot also includes a ball-milled and shock compacted (BM-SC) $TiNiSn_{0.95}Sb_{0.05}$ sample, with D ≤ 0.05 µm and a remarkably low κ_L for a half-Heusler alloy, ($\kappa_L \leq 4$ W $m^{-1}K^{-1}$). The line is a guide to the eye

Conclusions

Two different phonon scattering mechanisms in the $TiNiSn_{1-x}Sb_x$ and the $Ti_{1-y}Zr_yNiSn_{0.95}Sb_{0.05}$ series of half-Heusler alloys are presented. In the $TiNiSn_{1-x}Sb_x$ series, there is a direct correlation between the average grain diameter (D) and the lattice thermal conductivity (κ_L). Phonon boundary scattering is believed to be the prominent scattering mechanism when the grain size is about 10 µm or less. In the second series of $Ti_{1-y}Zr_yNiSn_{0.95}Sb_{0.05}$ compounds, the average grain size, D is observed to be greater than 50 µm. The reduction in κ_L is attributed to mass fluctuation scattering. Our experimental results are in good agreement with the theoretical predictions of Goldsmid *et al.*,[Error! Bookmark not defined.,Error! Bookmark not defined.] on phonon boundary scattering in the half-Heusler alloys, establishing a dependence of lattice thermal conductivity on the grain size (D ≤ 10 µm) in the half-Heusler alloys.

Acknowledgments

The research at Clemson University was funded in part by ONR DEPSCoR program ONR #N00014-03-0787 and SC EPSCoR/Clemson University cost share.

Notes and references

1 "Electronic Refrigeration", by H.J. Goldsmid.
2 Proceedings of the 1997 Materials Research Society **Volume 478,** Warrendale, PA**,** *Thermoelectric Materials -New Directions and Approaches* Edited by: Terry M. Tritt, M. Kanatzidis, G. Mahan and H. B. Lyon, Jr.
3 Proceedings of 1998 Materials Research Society **Volume 545,** Warrendale, PA, New Materials for Small Scale Thermoelectric Refrigeration and Power Generation Applications, Edited by: Terry M. Tritt, M. Kanatzidis, G. Mahan and H. B. Lyon, Jr.
4 H.J. Goldsmid, Thermoelectric Refrigeration, Prenum Press, 1964.
5 Tritt, T.M., "Holey and Unholey Semiconductors", *Science* Vol. **283**, No. 5403 (1999) pp. 804-805.
6 G. D. Mahan, J. Appl. Phys. **65** (4) 1578 (1989).
7 S. Bhattacharya, Terry M. Tritt, Y.Xia, V. Ponnambalam, S.J.Poon and N. Thadhani, Appl. Phys. Lett **81**, 43 (2002).
8 T. M Tritt, S. Bhattacharya, Y. Xia, V. Ponnambalam, S. J. Poon and N. Thadhani, Conference Proceedings, 27th International Conference on Thermal Conductivity *27*/ Thermal expansion *15,(ICTC27)* p 17 (2003)
9 W. Jeitschko, Metall.Trans.**1**, 3159 (1970).
10 T.T.M. Palstra, G.J. Nieuwenhuys, R.F.M.Vlastuin, J.A.Mydosh and K.H.J.Buschow, J. Appl. Phys. **63**, 4279 (1988).
11 S. Bhattacharya, A.L. Pope, R.T. Littleton, Terry M. Tritt, V. Ponnambalam, Y.Xia, , and S.J. Poon , Appl. Phys. Lett. **77**, 2476 (2000).
12 Q. Shen, L. Chen, T. Goto, T. Hirai, J. Yang, G.P. Meisner and C. Uher; Appl. Phys. Lett. **79**, 4165 (2001).
13 S. R. Culp, S. J. Poon, N. Hickman, T. M. Tritt, J. Blumm, Appl. Phys. Lett. **88**, 042106 (2006)
14 A. L. Pope, R. T. Littleton, and T. M. Tritt, Rev. Sci. Instrum. **72**, 3129 (2001).

15 'Thermal conductivity of semiconductors' by Nolas and Goldsmid, p. 105, in Thermal conductivity, theory, properties and applications, edited by Terry M. Tritt, Kluwer Academic/Plenum Press
16 Heinrich Hohl, Art P. Ramirez, Claudia Goldman, Gabriele Ernst, Bernd Wölfing and Ernst Bucher, J. Phys.: Condens. Matter **11**, 1697 (1999)